THE JOURNAL OF BIOLOGICAL CHEMISTRY VOL. 286, NO. 11, pp. 9468–9476, March 18, 2011

A Microarray-based Approach Identifies ADP Ribosylation Factor-like Protein 2 as a Target of microRNA-16*[S]

Received for publication, August 24, 2010, and in revised form, December 2, 2010 Published, JBC Papers in Press, January 3, 2011, DOI 10.1074/jbc.M110.178335

Kehui Wang, Peng Li, Yanye Dong, Xing Cai, Dongxia Hou, Jigang Guo, Yuan Yin, Yujing Zhang, Jing Li, Hongwei Liang, Bowen Yu, Jiangning Chen, Ke Zen[1], Junfeng Zhang[2], Chen-Yu Zhang[3], and Xi Chen[4]

From the Jiangsu Diabetes Center, State Key Laboratory of Pharmaceutical Biotechnology, School of Life Sciences, Nanjing University, Nanjing, Jiangsu 210093, China

microRNAs (miRNAs) are generally thought to negatively regulate the expression of their target genes by mRNA degradation or by translation repression. Here we show an efficient way to identify miRNA target genes by screening alterations in global mRNA levels following changes in miRNA levels. In this study, we used mRNA microarrays to measure global mRNA expression in three cell lines with increased or decreased levels of miR-16 and performed bioinformatics analysis based on multiple target prediction algorithms. For further investigation among the predicted miR-16 target genes, we selected genes that show an expression pattern opposite to that of miR-16. One of the candidate target genes that may interact with miR-16, ADP-ribosylation factor-like protein 2 (ARL2), was further investigated. First, ARL2 was deduced to be an ideal miR-16 target by computational predictions. Second, ARL2 mRNA and protein levels were significantly abolished by treatment with miR-16 precursors, whereas a miR-16 inhibitor increased ARL2 mRNA and protein levels. Third, a luciferase reporter assay confirmed that miR-16 directly recognizes the 3′-untranslated region (3′-UTR) of ARL2. Finally, we showed that miR-16 could regulate proliferation and induce a significant G0/G1 cell cycle arrest, which was due at least in part, to the down-regulation of ARL2. In summary, the present study suggests that integrating global mRNA profiling and bioinformatics tools may provide the basis for further investigation of the potential targets of a given miRNA. These results also illustrate a novel function of miR-16 targeting ARL2 in modulating proliferation and cell cycle progression.

Recently, a new class of RNA regulatory genes known as microRNAs (miRNAs)[5] has introduced a new layer of gene regulation in eukaryotes (1, 2). miRNAs are endogenous non-coding RNAs consisting of 19–24 nucleotides. They play an important role in the negative regulation of gene expression by base pairing to complementary sites on target messenger RNAs (mRNAs), thus causing a block in translation or triggering the degradation of the target mRNAs (1, 2). miRNAs are now reported to play fundamental roles in a wide variety of biological processes including developmental timing, apoptosis, proliferation, differentiation, organ development, carcinogenesis, immune response, and energy metabolism (1, 2).

miR-16 is a miRNA that has been extensively investigated. A study by Calin *et al.* (3) revealed that miR-15a and miR-16–1 are down-regulated in the majority of chronic lymphocytic leukemia cases, implying that they may function as tumor suppressors in this disease. Cimmino *et al.* (4) further showed that miR-15a/miR-16 expression is inversely correlated to B cell lymphoma 2 (BCL2) expression, and BCL2 repression by these miRNAs induces spontaneous apoptosis in a leukemic cell line model. Moreover, it was shown that the miR-16 family negatively regulates cell cycle progression from G0/G1 to S by silencing multiple cell cycle genes including CCND1, CCND3, CCNE1, CDK6, CARD10, and CDC27 (5–7). Furthermore, Jing *et al.* (8) provided evidence that miR-16 is involved in controlling the turnover of AU-rich element-containing mRNA (ARE-RNA), suggesting that miRNAs may play an important role in ARE-mediated mRNA instability. Taken together, miR-16 is involved in the regulation of basal biological processes including cell cycle arrest, apoptosis, and tumorigenesis.

In the present study, we identified a large number of transcripts regulated by miR-16 directly or indirectly. We accomplished this by overexpressing or knocking down miR-16 in several cell lines and measuring global mRNA levels through microarray platforms. We identified ADP-ribosylation factor-like protein 2 (ARL2) among these candidate targets as a direct target of miR-16. The mechanism through which miR-16 executes its functions was also investigated in this study.

EXPERIMENTAL PROCEDURES

Cells, Reagents, and Antibodies—Human lung adenocarcinoma A549 cells, human embryonic kidney 293A cells, and human breast cancer MCF7 cells were purchased from the China Cell Culture Center (Shanghai, China). 293A cells were cultured in RPMI 1640 medium (Invitrogen) supplemented with 10% fetal bovine serum (FBS) (Invitrogen). A549 and MCF7 cells were maintained in DMEM medium (Invitrogen) supplemented with 10% FBS. Cells were grown at 37 °C in a

* This work was supported by Grants from the National Natural Science Foundation of China (Nos. 90813035, 81070653, 30890044, 30771036, 30772484, 30725008, 30890032, 31071232, 90608010), National Basic Research Program of China (973 Program) (Nos. 2006CB503908, 2006CB503909, 2007CB815701, 2007CB815703, 2007CB815705, 2007CB815804), the Chinese 863 program (2006AA02Z177, 2006AA10A121), the "111" Project, the Chinese Academy of Science (GJHZ0701-6, KSCX2-YWN-023), and the Natural Science Foundation of Jiangsu Province (No. BK2006714).

[S] The on-line version of this article (available at http://www.jbc.org) contains supplemental Table S1.

[1] To whom correspondence may be addressed. E-mail: kzen@nju.edu.cn.
[2] To whom correspondence may be addressed. E-mail: jfzhang@nju.edu.cn.
[3] To whom correspondence may be addressed. E-mail: cyzhang@nju.edu.cn.
[4] To whom correspondence may be addressed. E-mail: xichensunny@gmail.com.

[5] The abbreviations used are: miRNA, microRNA; UTR, untranslated region; ARL2, ADP-ribosylation factor-like protein 2; ncRNA, noncoding RNA.

humidified atmosphere with 5% CO_2. Synthetic RNA molecules, including pre-miR-16, anti-miR-16, and scrambled noncoding RNA (ncRNA), were purchased from Ambion (Austin, TX). Anti-ARL2 (ab3391) and anti-GAPDH (6C5) antibodies were purchased from Abcam Biotechnology (Cambridge, UK) and Santa Cruz Biotechnology, respectively.

Overexpression or Knockdown of miR-16—miR-16 overexpression was achieved by transfecting cells with pre-miR-16 (synthetic RNA oligonucleotide mimicking miR-16 precursors), while miR-16 knockdown was achieved by transfecting cells with anti-miR-16 (chemically modified antisense oligonucleotide designed to specifically target against mature miR-16). ncRNA served as negative control. A549, 293A, and MCF7 cells were seeded onto 6-well plates or 60-mm dishes and were transfected the following day using Lipofectamine 2000 (Invitrogen), according to the manufacturer's instructions. For each well, equal doses (200 pmol) of scrambled ncRNA, pre-miR-16, or anti-miR-16 were added. Cells were harvested 24 h after transfection.

RNA Isolation and Quantitative RT-PCR—Total RNA was extracted from the cultured cells using TRIzol Reagent (Invitrogen) according to the manufacturer's instructions. For quantitative RT-PCR analysis of ARL2 and β-actin, 1 μg of total RNA was reverse transcribed to cDNA with oligdT and Thermoscript (TaKaRa, Dalian, China). Real-time PCR for ARL2 and β-actin was performed on an Applied Biosystems 7300 Sequence Detection System (Applied Biosystems, Foster City) using SYBR green dye (Invitrogen). A 20-μl PCR reaction was used and included 1 μl of RT product, 1× QuantiTect SYBR green PCR Master Mix, and 0.5 μM sense and antisense primers. The reactions were incubated in a 96-well plate at 95 °C for 5 min followed by 40 cycles of 95 °C for 30 s, 60 °C for 30 s, and 72 °C for 30 s. All reactions were run in triplicate. After the reactions were run, the threshold cycles (C_T) were determined using fixed threshold settings. The sequences of the sense and antisense primers used for amplification of ARL2 and β-actin were as follows: ARL2 (sense): 5′-GGGAGGACATCGACACCA-3′; ARL2 (antisense): 5′-AGGACCGCAGGGACTTCT-3′; β-actin (sense): 5′-AGGGAAATCGTGCGTGAC-3′; and β-actin (antisense): 5′-CGCTCATTGCCGATAGTG-3′.

Assays to quantify mature miR-16 were carried out using Taqman microRNA probes (Applied Biosystems) according to previous publications (9, 10). Briefly, 5 μl of total RNA was reverse-transcribed to cDNA using AMV reverse transcriptase (TaKaRa, Dalian, China) and a stem-loop RT primer (Applied Biosystems). Real-time PCR was performed using a TaqMan PCR kit on an Applied Biosystems 7300 Sequence Detection System (Applied Biosystems). All reactions, including no-template controls, were run in triplicate. After the reactions, the C_T values were determined using fixed threshold settings. In the experiments presented here, miRNA expression in cells was normalized to U6 snRNA, similar to many other reports (11). The relative amount of miR-16 to internal control U6 was calculated with the equation $2^{-\Delta CT}$, in which $\Delta C_T = C_{T\,miR\text{-}16} - C_{T\,U6}$.

Microarray Procedures—The commercially available 22K Human Genome Array was purchased from CapitalBio Corporation (Beijing, China). Labeling, hybridization, washing, and scanning were performed according to the standard operating procedure of CapitalBio Corporation. Briefly, total RNA was used to synthesize cDNA in an *in vitro* transcription reaction. cDNA was fluorescently labeled by Cy5 or Cy3-CPT with Klenow enzyme. After hybridization, the microarray was washed with two consecutive washing solutions (0.2% SDS and 2× SSC at 42 °C for 5 min, and 0.2% SSC for 5 min at room temperature). Subsequently, these arrays were scanned with a LuxScan 10KA confocal laser scanner (CapitalBio Corp.), and the obtained images were analyzed using LuxScan Version 3.0 (CapitalBio Corp.), which employed the LOWESS normalization method.

miR-16 Target Prediction—The analysis of miRNA predicted targets was determined with the algorithms from TargetScan (12), PicTar (13), and miRanda (14).

Western Blotting—ARL2 protein level was quantified by Western blot analysis of whole cell extracts using antibodies against ARL2. These samples were normalized by blotting with an antibody against GAPDH.

Plasmid Construction and Luciferase Assay—The entire human ARL2 3′-untranslated region (3′-UTR) was amplified by PCR using human genomic DNA as a template. The PCR products were inserted into the p-MIR-report plasmid (Ambion). Efficient insertion was confirmed by sequencing. For luciferase reporter assays, cells were cultured in 6-well plates, and each well was transfected with 2 μg of firefly luciferase reporter plasmid, 2 μg of β-galactosidase expression vector (Ambion), and equal amounts of scrambled ncRNA, pre-miR-16, or anti-miR-16 using Lipofectamine 2000 (Invitrogen). The β-galactosidase vector was used as a transfection control. At 24 h post-transfection, cells were assayed using luciferase assay kits (Promega, Madison, WI). Data depicted are representative of three independent experiments performed on different days.

siRNA Interference Assay—Three siRNA sequences targeting different sites of human ARL2 cDNA were designed and synthesized by Invitrogen. A scrambled siRNA (Stealth™ RNAi negative control kit, Invitrogen) that could not target human ARL2 cDNA was included as a negative control. siRNA sequences were as follows: siRNA-1: 5′-UGCGCUGUCCACUACCCAGAUGAGG-3′ (sense); 5′-CCUCAUCUGGGUAGUGGACAGCGCA-3′ (antisense); siRNA-2: 5′-UCUUCAGGAUGGUUGUCUUUCCAGC-3′ (sense); 5′-GCUGGAAAGACAACCAUCCUGAAGA-3′ (antisense); siRNA-3; 5′-UGUUCAGCUUGAAUCCUCGGUGCUC-3′ (sense), 5′-GAGCACCGAGGAUUCAAGUCGAACA-3′ (antisense).

siRNA was transfected into A549 cells using Lipofectamine 2000 (Invitrogen) according to the manufacturer's instructions. Total RNA was isolated at 24 h post-transfection. The expression level of ARL2 mRNA was assessed by quantitative RT-PCR. The sequence with the best interfering effect (named siRNA-3) was selected and used in further studies.

Cell Viability Assay—A549 cells were plated at 2.5×10^3 cells per well in 96-well plates and incubated overnight in DMEM medium supplemented with 10% FBS. After transfection, 20 μl of 3-(4,5-dimethylthiazol-2-yl)-2,5-diphenyl tetrazolium bromide (MTT) (5 mg/ml) was added into a corresponding test well and incubated for 4 h. The supernatant was then discarded, and 200 μl of DMSO was added to each well to dissolve the

precipitate. Absorbance (*A*) was measured at a wavelength of 570 nm.

Cell Migration Assay—The migration ability of A549 cells was tested in a Transwell Boyden Chamber (6.5 mm, Costar, Cambridge, MA). The polycarbonate membranes (8-μm pore size) on the bottom of the upper compartment of the Transwells were coated with a 0.1% gelatin matrix. Cells treated with ncRNA, pre-miR-16, or siRNA for 6 h were suspended in serum-free DMEM culture medium at a concentration of 4×10^5 cells/ml and then added to the upper chamber (4×10^4 cells/well). Simultaneously, 0.5 ml of DMEM with 10% FBS was added to the lower compartment, and the Transwell-containing plates were incubated for 8 h in a 5% CO_2 atmosphere saturated with H_2O. At the end of the incubation, cells that had entered the lower surface of the filter membrane (migrant cells) were fixed with 90% ethanol for 15 min at room temperature, washed three times with distilled water, and stained with 0.1% crystal violet in 0.1 M borate and 2% ethanol for 15 min at room temperature. Cells remaining on the upper surface of the filter membrane (non-migrant) were scraped off gently with a cotton swab. Images of migrant cells were captured by a photomicroscope (BX51, Olympus, Japan). Cell migration was quantified by blind counting of the migrated cells on the lower surface of the membrane with five fields per chamber.

Cell Cycle Assay—Cells were harvested, washed once with PBS, and fixed in 70% ethanol overnight. Staining for DNA content was performed with 50 mg/ml propidium iodide and 1 mg/ml RNase A for 30 min. Analysis was performed on a fluorescence-activated cell-sorting (FACS) flow cytometer (BD Biosciences, San Jose, CA) with Cell Quest Pro software. Cell-cycle modeling was performed with Modfit 3.0 software (Verity Software House, Topsham, ME).

Statistical Analysis—All photo-images of Western blotting and semi-quantitative RT-PCR were representative of at least three independent experiments. Quantitative RT-PCR, luciferase reporter assay, and cell migration assays were performed in triplicate, and each experiment was repeated three to five times. Data shown are presented as mean ± S.D. of at least three independent experiments. Statistical significance was considered at $p < 0.05$ using the Student's *t* test.

RESULTS

Identification of Transcripts Regulated by miR-16 by Microarray Analysis—We first screened the expression levels of miR-16 in A549, 293A, and MCF7 cells. Our results showed that miR-16 can be readily detected in all cells (Fig. 1, *A* and *B*), consistent with the fact that miR-16 is ubiquitously expressed in many mammalian tissues and cells.

miRNAs are generally thought to negatively regulate the expression of their targets by mRNA degradation or by translational repression (1, 2). Therefore, if a given miRNA can mediate the degradation of targeted mRNAs, this miRNA and its targets should have expression patterns in the opposite directions. In light of this mode of miRNA action, we postulated that candidate miRNAs affecting transcript levels could be deduced from mRNA microarray expression profiles. We therefore transfected A549, 293A, and MCF7 cells with equal doses of scrambled ncRNA, pre-miR-16, or anti-miR-16. We then surveyed potential genes that were inversely expressed relative to miR-16 using microarray analysis. As shown in Fig. 1*C*, the expression of miR-16 was abolished by the introduction of anti-miR-16, whereas pre-miR-16 significantly increased miR-16 levels in A549, 293A, and MCF7 cells. The mRNA microarray profiles clearly showed different mRNA expression patterns among pre-miR-16- and anti-miR-16-transfected cells compared with ncRNA-transfected cells. In total, 115, 389, and 188 genes were down-regulated (mean fold change <0.66) in miR-16-overexpressed A549, 293A, and MCF7 cells, respectively, while 45, 218, and 34 genes were up-regulated (mean fold change > 1.5) in miR-16-down-regulated A549, 293A, and MCF7 cells, respectively (Fig. 1*D*). To reduce the false positives and obtain a more accurate assessment of the genuine miR-16 targets, only the mRNAs that showed consistent expression patterns in all three cell lines were considered as candidate miR-16 targets. A set of 26 down-regulated and 6 up-regulated genes in these cells were identified as candidate miR-16 targets (Fig. 1*D* and Tables 1 and 2).

Enrichment of miR-16 Target Genes among Differentially Expressed Genes—We next calculated whether the differentially regulated genes were predicted miR-16 targets using three widely used programs: TargetScan, PicTar, and MiRanda (12–14). Because individual computer-aided algorithms can generate a high number of false positives, the combination of these three approaches provided a more accurate assessment of the genuine miRNA targets than a single approach would. Therefore, these algorithms were used in combination to provide the highest probability of target identification, and only the genes predicted as miR-16 targets by at least two of the above-mentioned algorithms were considered positive. Among the list of the 26 down-regulated genes obtained from miR-16 overexpression, 13 were predicted as miR-16 targets (Table 3). From the six up-regulated genes obtained from miR-16 knockdown, 2 genes were identified as miR-16 targets (Table 3). In contrast, out of the 423 unchanged genes in the three cell lines ($0.95 <$ mean fold change < 1.05), only 15 were identified as predicted miR-16 targets (Table 3). Moreover, seven genes showed the same direction of change with miR-16 (up-regulation upon overexpression of miR-16, mean fold change > 1.5; or down-regulation upon knockdown of miR-16, mean fold change < 0.66); however, none were identified as predicted targets of miR-16 (Table 3). These results indicate that the predicted miR-16 targets are more frequently found among genes with expression patterns opposite to that of miR-16, further indicating that these relationships may be functional miRNA-target combinations.

The ARL2 3′-UTR Contains Four Putative Target Sites for miR-16—As noted, ARL2 was the most significantly down-regulated gene in all three cell lines when miR-16 was overexpressed (Table 1). Intriguingly, ARL2 was identified as a candidate target of miR-16 by all three programs (supplemental Table S1). The predicted interaction between miR-16 and its target sites in the ARL2 3′-UTR is illustrated in Fig. 2*A*. As shown in this figure, there are four potential target sites in the 3′-UTR of ARL2 for miR-16. The minimum free energy values of these hybrids are −14.2, −15.8, −15.5, and −14.8 kcal/mol,

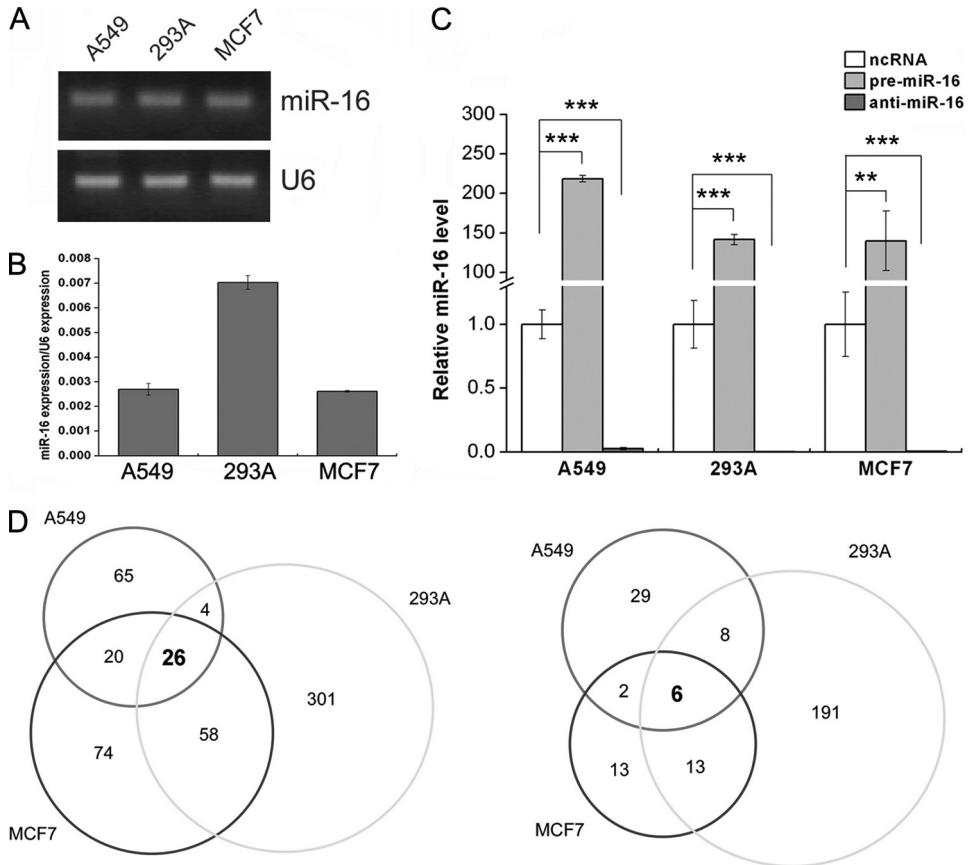

FIGURE 1. **Differentially regulated genes in cells with increased or decreased expression of miR-16.** *A*, semi-quantitative RT-PCR analysis of miR-16 expression levels in A549, 293A, and MCF7 cells. *B*, quantitative RT-PCR analysis of miR-16 relative expression normalized to U6 RNA in A549, 293A, and MCF7 cells. The results are presented as the mean ± S.D. of three independent experiments. *C*, overexpression or knockdown of miR-16. A549, 293A, and MCF7 cells were seeded on 6-well plates and transfected the following day with Lipofectamine 2000. For each well, 200 pmol of scrambled ncRNA, pre-miR-16, or anti-miR-16 were added. The intercellular levels of miR-16 were evaluated by quantitative RT-PCR at 24 h post-transfection. For comparison, the expression levels of miR-16 in ncRNA-transfected cells were arbitrarily set at 1. The *y* axis shows arbitrary units representing relative miR-16 expression levels. The results are presented as the mean ± S.D. of three independent experiments (**, $p < 0.01$; ***, $p < 0.001$). *D*, Venn diagram of the overlap of altered genes in three cell lines with increased or decreased expression of miR-16. Results after gain and loss of miR-16 function are presented in separate Venn diagrams (*left*: gain of function of miR-16; *right*: loss of function of miR-16). The genes differentially expressed in A549, 293A, and MCF7 cells are depicted in the three overlapping *circles*. *Numbers* in overlapping areas indicate the number of mRNAs that belong to the intersecting sets. The number of mRNAs altered in all three cell lines is indicated in *bold*.

TABLE 1

mRNAs down-regulated in pre-miR-16-transfected A549, 293A, and MCF7 cells compared with ncRNA-transfected cells

Gene name	A549	293A	MCF7	Mean fold-change
ARL2	0.405	0.164	0.413	0.327
CDS2	0.426	0.404	0.417	0.415
SLC35A4	0.464	0.346	0.493	0.434
MAP7	0.568	0.192	0.552	0.438
C1orf2	0.533	0.344	0.524	0.467
RARS	0.611	0.276	0.549	0.479
SPRYD3	0.539	0.424	0.487	0.483
VTI1B	0.480	0.373	0.605	0.486
ANAPC13	0.566	0.455	0.483	0.501
RNF111	0.592	0.406	0.51	0.502
ALG3	0.542	0.444	0.578	0.521
XKR8	0.661	0.390	0.531	0.527
ARG2	0.416	0.556	0.638	0.537
MRPL20	0.548	0.446	0.629	0.541
RPS6KA3	0.598	0.429	0.617	0.548
RTN4	0.631	0.478	0.550	0.553
MMS19	0.620	0.494	0.579	0.564
CCNE1	0.572	0.527	0.615	0.571
TOMM34	0.629	0.483	0.620	0.577
CHPT1	0.613	0.553	0.603	0.590
KIAA0746	0.578	0.585	0.640	0.601
CXorf40A	0.562	0.631	0.610	0.601
NECAP1	0.620	0.528	0.670	0.606
PPP1R11	0.663	0.515	0.660	0.613
KIF1B	0.57	0.65	0.624	0.615
SMURF2	0.643	0.658	0.561	0.621

TABLE 2

mRNAs up-regulated in anti-miR-16-transfected A549, 293A, and MCF7 cells compared with ncRNA-transfected cells

Gene name	A549	293A	MCF7	Mean fold-change
SNRPC	1.683	3.433	1.549	2.222
ASPH	1.808	2.683	1.536	2.009
GNB1	1.665	2.185	1.716	1.856
COMMD10	1.496	2.359	1.549	1.801
NARF	1.806	1.863	1.690	1.786
UBE2V1	1.704	1.604	1.504	1.604

determined by RNA hybrid analysis (15), which are well within the range of authentic miRNA-target pairs (Fig. 2*A*). Moreover, perfect base pairing between the "seeds" (the core sequence that encompasses the first 2–8 bases of the mature miRNA) and cognate targets (Fig. 2*A*) was noted, and the miR-16 binding sequences at the ARL2 3′-UTR are highly conserved across species (Fig. 2*B*). The common criteria to decide whether a transcript is a target for a miRNA is base pairing between the "seed" and target, strict interspecies conservation of the miRNA binding sequence, and an inverse correlation between the miRNA expression levels and its target levels. Because miR-16 targeting ARL2 fulfills these criteria, we next focused on studying the role of miR-16 in regulating ARL2 expression.

TABLE 3
Genes showing expression patterns opposite to that of miR-16 are enriched in miR-16 target genes

		TargetScan	PicTar	miRanda	At least one algorithm	More than one algorithm	*p* value
Group 1	Down-regulated genes upon overexpression of miR-16 (26)	13	10	12	14	13	0.000495[a]
Group 2	Up-regulated genes upon knockdown of miR-16 (6)	2	2	3	3	2	0.004581[b]
Group 3	Genes showing concordant direction of the change with miR-16 (7)	0	0	1	1	0	0.8889[c]
Group 4	Unchanged genes (423)	16	16	38	47	15	

[a] Group 1 vs. Group 4.
[b] Group 2 vs. Group 4.
[c] Group 3 vs. Group 4.

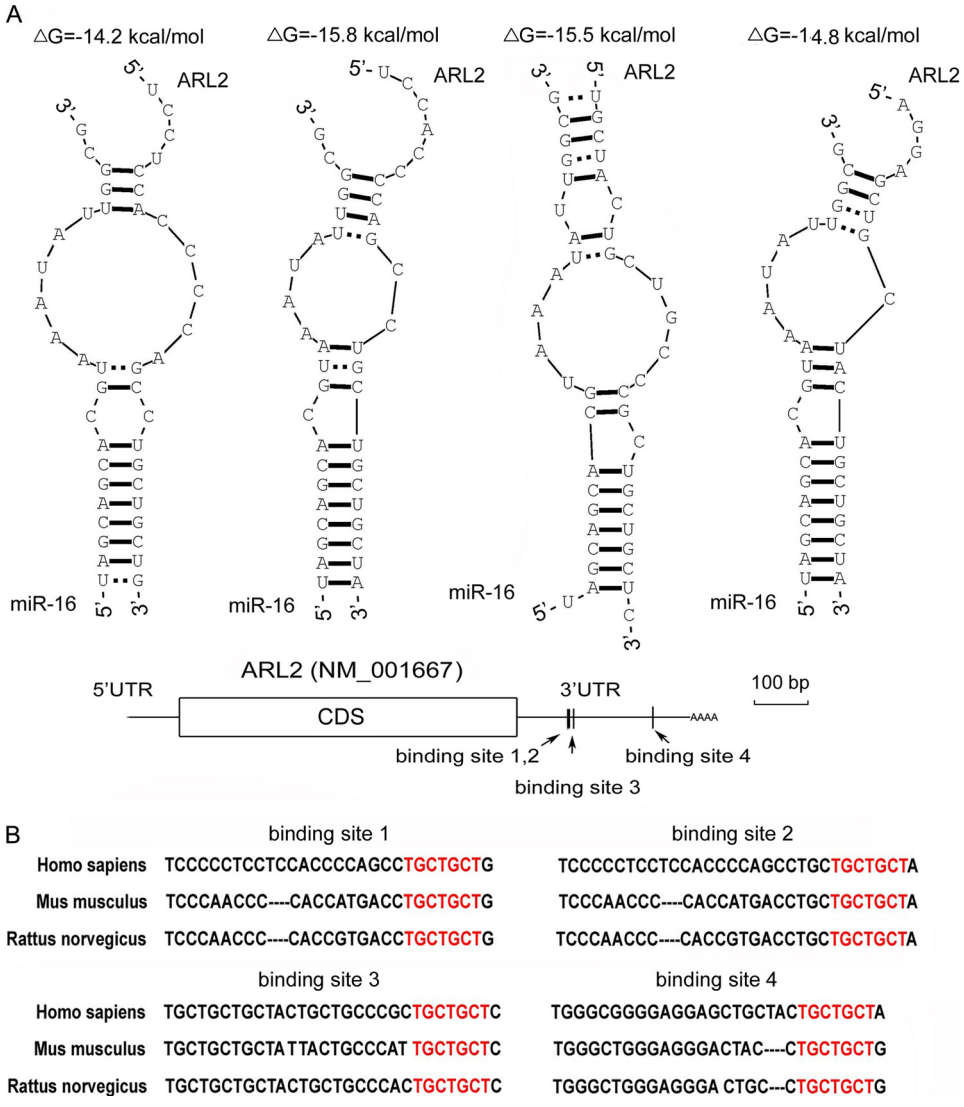

FIGURE 2. **Identification of conserved miR-16 binding sites within the ARL2 3′ UTR.** *A*, schematic description of the hypothesized duplexes formed by interactions between the ARL2 3′-UTR binding sites and miR-16. Each binding site is numbered, and the predicted structure of each base-paired hybrid is diagrammed. Paired bases are indicated by a *black oval*, and G:U pairs are indicated by *two dots*. The predicted free energy of each hybrid is indicated. *B*, sequence alignment of the putative miR-16 binding sites across species. The seed complementary sites are marked in *red*, and all nucleotides in these regions are completely conserved in several species including human, mouse, and rat.

Down-regulation of ARL2 Expression by miR-16—Microarray analysis showed that miR-16 was able to regulate the steady-state level of ARL2 mRNA (Table 1). We further validated this result by performing a quantitative RT-PCR assay with the same RNA preparations as discussed previously. A549, 293A, and MCF7 cells were transfected with ncRNA, pre-miR-16, or anti-miR-16 and analyzed for the expression of ARL2 mRNA by quantitative RT-PCR at 24 h post-transfection. All cells transfected with pre-miR-16 showed reduced levels of ARL2 mRNA relative to the cells transfected with ncRNA. In contrast, anti-miR-16 significantly increased the expression levels of ARL2 mRNA in these three cell lines (Fig. 3*A*).

To determine whether the overexpression or knockdown of miR-16 had an impact on ARL2 protein expression, we repeated the above-mentioned experiments and determined the expression of ARL2 protein by Western blotting at 24 h

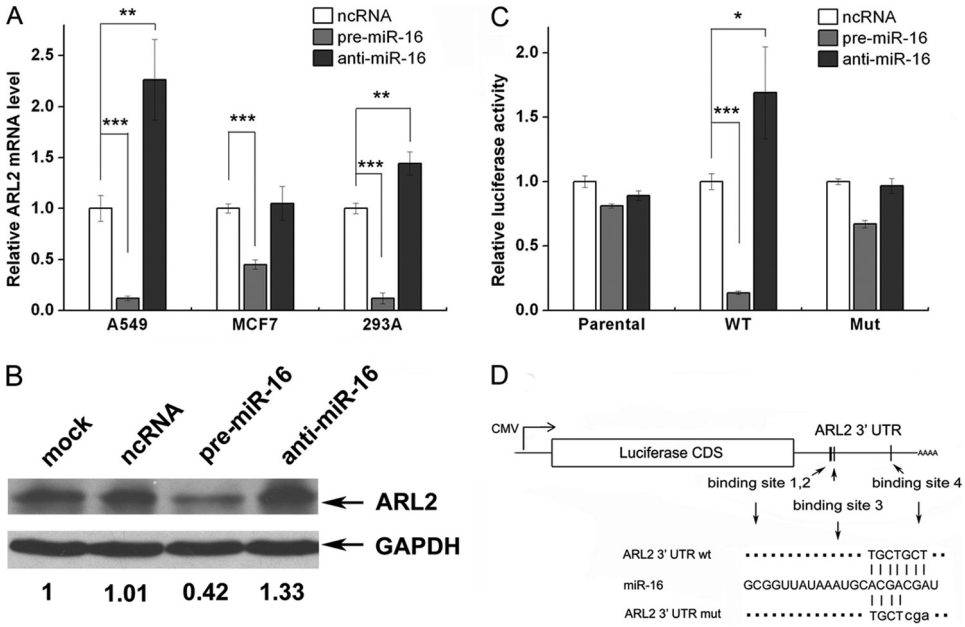

FIGURE 3. **Regulation of ARL2 expression by miR-16 at both the transcript and protein levels.** *A*, quantitative RT-PCR analysis of ARL2 mRNA levels in A549, 293A, and MCF7 cells treated with scrambled ncRNA, pre-miR-16, or anti-miR-16. For comparison, the expression levels of ARL2 mRNA in ncRNA-transfected cells were arbitrarily set at 1. The *y* axis shows arbitrary units representing relative ARL2 mRNA levels. The results are presented as the mean ± S.D. of three independent experiments (**, $p < 0.01$; ***, $p < 0.001$). *B*, Western blot analysis of ARL2 protein levels in A549 cells untreated or treated with scrambled ncRNA, pre-miR-16, or anti-miR-16. Results are representative data from three independent experiments. Pictures of the Western blot assay were analyzed using Bandscan software, and a statistical analysis is present below. *C*, direct recognition of the ARL2 3′-UTR by miR-16. Firefly luciferase reporters containing either wt or mut ARL2 3′-UTR were co-transfected into A549 cells with scrambled ncRNA, pre-miR-16, or anti-miR-16. The parental luciferase plasmid was also transfected as a control. At 24 h post-transfection, cells were assayed using luciferase assay kits. For comparison, the luciferase activity in ncRNA-transfected cells was arbitrarily set at 1. The *y* axis shows arbitrary units representing relative luciferase activity. The results are presented as the mean ± S.D. of three independent experiments (*, $p < 0.05$; ***, $p < 0.001$). *D*, diagram of the luciferase reporter plasmid carrying the firefly luciferase coding sequence attached to the human ARL2 3′-UTR with either wild-type (wt) or mutant (mut) miR-16 binding sites (the sequence that interacts with the 2–4 bases of miR-16 were mutated).

post-transfection. As shown in Fig. 3*B*, the expression of ARL2 protein was significantly abolished by the introduction of pre-miR-16, whereas cells transfected with scrambled ncRNA maintained a considerable amount of ARL2 protein. In contrast, anti-miR-16 significantly increased ARL2 protein in A549 cells. Moreover, the ARL2 protein expression was inversely correlated to miR-16 in both 293A and MCF7 cells (data not shown). These results demonstrate that miR-16 regulates the expression of ARL2 at both the transcript and protein levels.

ARL2 Is a Direct Target of miR-16—To determine whether the negative regulatory effects of miR-16 on ARL2 expression were mediated through binding to the presumed complementary sites at the 3′-UTR of ARL2, we fused the entire ARL2 3′-UTR into a downstream position of the firefly luciferase reporter plasmid. The resulting plasmid was introduced into A549 cells combined with a transfection control plasmid (β-gal) and pre-miR-16, anti-miR-16, or scrambled ncRNA. As expected, overexpression of miR-16 resulted in a significant decrease in the luciferase reporter activity (normalized against β-gal activity) compared with the treatment with scrambled ncRNA; however, inhibition of miR-16 resulted in a significant increase in reporter activity (Fig. 3*C*). The observed alterations in luciferase activity were specific, as co-transfection of A549 cells with the parental luciferase plasmid (without the ARL2 3′-UTR) and pre-miR-16 or anti-miR-16 did not affect luciferase reporter activity (Fig. 3*C*). Furthermore, we introduced a point mutation into the corresponding seed complementary sites in the ARL2 3′-UTR to eliminate the predicted binding by miR-16 (Fig. 3*D*). As shown in Fig. 3*C*, mutations in the seed complementary sites almost fully rescued the repression of reporter activity by pre-miR-16. Also, the mutant luciferase reporter was unaffected by miR-16 inhibition in A549 cells. This suggests that these binding sites strongly contribute to the miRNA:mRNA interaction that mediates the post-transcriptional inhibition of ARL2 expression. Moreover, similar results were observed in experiments carried out in 293A and MCF7 cells (data not shown). In conclusion, our results demonstrate that miR-16 directly recognizes the 3′-UTR of the ARL2 transcript to down-regulate its expression.

The Role of miR-16 and ARL2 in Cell Cycle and Proliferation—To investigate the cellular phenotypes triggered by miR-16 targeting ARL2, A549 cells were transfected with miR-16 precursors or siRNA against ARL2 and analyzed for the changes of migration, proliferation, and cell cycle arrest. Cells transfected with ncRNA or control siRNA served as controls. Efficient interference of ARL2 expression is shown in Fig. 4, *A* and *B*.

We assessed the role of miR-16 on cell migration by Transwell assay. As shown in Fig. 4*C*, the migration rate of A549 cells transfected with pre-miR-16 was significantly decreased compared with control cells. However, no differences were observed in migration rates between the cells transfected with negative control siRNA or siRNA against ARL2. These results suggest that miR-16 could modulate cell migration by down-regulating genes other than ARL2.

The proliferation rates of A549 cells with increased or decreased expression of miR-16 were determined via MTT

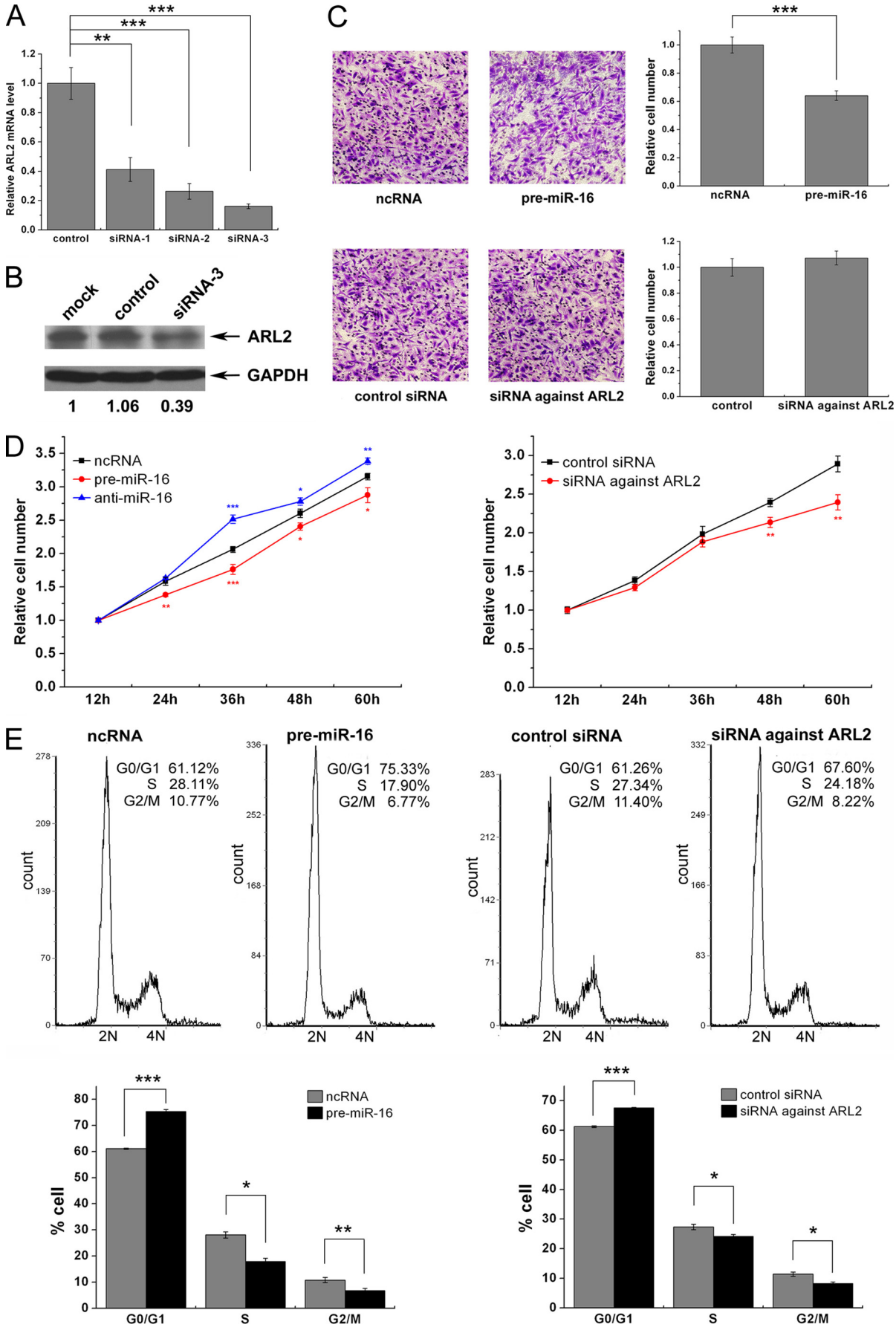
A
Relative ARL2 mRNA level
control
siRNA-1
siRNA-2
siRNA-3
B
mock
control
siRNA-3
ARL2
GAPDH
1
1.06
0.39
C
ncRNA
pre-miR-16
Relative cell number
control siRNA
siRNA against ARL2
D
ncRNA
pre-miR-16
anti-miR-16
Relative cell number
12h
24h
36h
48h
60h
control siRNA
siRNA against ARL2
E
ncRNA
G0/G1 61.12%
S 28.11%
G2/M 10.77%
pre-miR-16
G0/G1 75.33%
S 17.90%
G2/M 6.77%
control siRNA
G0/G1 61.26%
S 27.34%
G2/M 11.40%
siRNA against ARL2
G0/G1 67.60%
S 24.18%
G2/M 8.22%
count
2N
4N
% cell
G0/G1
S
G2/M

assay. Compared with ncRNA-transfected cells, cells transfected with anti-miR-16 proliferated at a significantly higher rate. In contrast, overexpression of miR-16 by transfection with pre-miR-16 resulted in significantly reduced proliferation (Fig. 4*D*). Furthermore, significant difference was observed in proliferation rates between the cells transfected with control siRNA and siRNA against ARL2. The results suggest that miR-16 might inhibit cell proliferation by silencing ARL2.

Finally, we investigated cell cycle distribution in cells with enhanced miR-16 or silenced ARL2 by flow cytometry analysis. Compared with cells transfected with ncRNA, cells transfected with pre-miR-16 triggered an accumulation of cells in the G0/G1 stage, whereas the numbers of cells in the S and G2/M phases decreased (Fig. 4*E*). The percentage of ncRNA-treated cells in the G0/G1 phase was 61.12 ± 0.22%, while transfection with pre-miR-16 resulted in 75.33 ± 0.85% of cells in the G0/G1 phase. The S phase fractions in control and pre-miR-16 groups were 28.11 ± 1/19% and 17.90 ± 1.27%, respectively, and the G2/M phase fractions in control and pre-miR-16 groups were 10.77 ± 1.01% and 6.78 ± 0.81%, respectively. Transfection with siRNA against ARL2 partially yielded the phenotype generated by overexpression of miR-16, but the effects were somewhat different, featured by a lower G0/G1 cell accumulation but a higher S and G2/M cell accumulation (Fig. 4*E*). In A549 cells, 61.26 ± 0.30% of the cell population went into arrest in the G0/G1 phase when ARL2 was interfered with siRNA, whereas 67.60 ± 0.17% of the control cells transfected with ncRNA were in this phase of the cell cycle. The S phase fractions in control and siRNA-treated groups were 27.34 ± 0.92% and 24.18 ± 0.67%, respectively, and the G2/M phase fractions in control- and siRNA-treated groups were 11.40 ± 0.73% and 8.22 ± 0.54%, respectively. Comparable results were also observed in 293A and MCF7 cells (data not shown). Taken together, our data suggests that miR-16 might negatively regulate cell cycle progression from the G0/G1 phase to the S phase by silencing ARL2.

DISCUSSION

Although the number of known miRNAs is continuously increasing, information regarding their precise cellular function remains limited. One of the main challenges in understanding the functions of miRNAs is to identify the genuine target genes of miRNAs. However, lack of reliable and specific methods for biological target validation hampers the full understanding of the mechanisms by which miRNAs execute their functions. Only a few miRNAs have thus far been assigned target mRNAs, and the conventional methodologies are still labor intensive. Therefore, novel approaches for target identification are required to overcome this limitation.

Animal miRNAs were originally believed to block translational processes without affecting transcript levels (1, 2); however, recent studies have suggested that they can also induce mRNA degradation or destabilization even in the absence of extensive base pairing to their targets (16–21). This was first clearly demonstrated by the observation that overexpression of a specific miRNA could reduce the expression of hundreds of mRNAs (16). Subsequently, the action of miRNAs on mRNA levels has been widely confirmed in other studies (17–20). A recent publication reported the impact of miRNAs on global mRNA and protein expression and showed that the regulation of protein-coding genes by miRNAs is quite similar at both the transcript and protein levels (21). Inspired by this mode of miRNA action, we postulated that the high-throughput mRNA microarray assays capable of detecting such effects at the mRNA level would provide a promising way to assist in miRNA target identification. Indeed, by globally screening the expression patterns of transcripts in several cell lines using microarray analysis, we found that a large number of transcripts change after miRNA transfection (Fig. 1 and Tables 1 and 2). To obtain a more accurate assessment of the genuine miR-16 targets, we combined bioinformatics programs to select candidate miR-16 targets from the differentially regulated genes. In contrast to unchanged gene expression and genes showing a similar direction of expression with miR-16, putative miRNA targets revealed significant enrichment in genes having expression patterns opposite to that of miR-16 (Table 3). These results suggest that many of these genes are genuine targets of miR-16 rather than genes secondarily regulated as part of the miRNA-mediated module controlled by the direct miRNA targets. Therefore, our strategies combining global gene expression analysis with bioinformatics prediction may provide additional confirmatory evidence to aid in miRNA target identification.

Among a panel of candidate targets that may interact with miR-16, ARL2, a 21-kDa GTPase belonging to the ADP-ribosylation factor (ARF) family (22, 23), was further experimentally validated as a miR-16 target. The reasons we focused on miR-16 targeting ARL2 include the following: (*a*) ARL2 was down-regulated most significantly in all three cell lines when miR-16 was overexpressed and (*b*) ARL2 was deduced to be an ideal miR-16 target by computational predictions. Indeed, through several biological approaches, we demonstrated that miR-16 regulates

FIGURE 4. **The role of miR-16 targeting ARL2 in cell cycle regulation.** *A*, selection of efficient siRNA against ARL2. Three siRNA sequences targeting different sites of human ARL2 cDNA and a scrambled control siRNA were transfected into A549 cells using Lipofectamine 2000. Total RNA was isolated at 24 h post-transfection. The expression levels of ARL2 mRNA were assessed by quantitative RT-PCR. The sequence with the best interfering effect (named siRNA-3) was selected and used in further studies (mean ± S.D.; **, $p < 0.01$; ***, $p < 0.001$). *B*, Western blot analysis of ARL2 protein levels in A549 cells untreated or treated with control siRNA or siRNA-3 at 48 h post-transfection. Results are representative data from three independent experiments. Pictures of the Western blot assay were analyzed using Bandscan software, and a statistical analysis is present below. *C*, Transwell analysis of A549 cells treated with equal doses of scrambled ncRNA or pre-miR-16 or equal doses of control siRNA or siRNA against ARL2. Representative images from three independent experiments are shown in the *left panel*, and a statistical analysis is present in the *right panel* (mean ± S.D.; ***, $p < 0.001$). *D*, MTT cell viability assay at 12, 24, 36, 48, and 60 h after transfection of A549 cells with equal doses of scrambled ncRNA, pre-miR-16, or anti-miR-16 or equal doses of control siRNA or siRNA against ARL2 (mean ± S.D.; *, $p < 0.05$; **, $p < 0.01$; ***, $p < 0.001$). *E*, overexpression of miR-16 and silencing of ARL2 by siRNA regulating cell cycle progression. A549 cells were transfected with equal doses of scrambled ncRNA or pre-miR-16 or equal doses of control siRNA or siRNA against ARL2. Cell cycle profiles were analyzed using flow cytometry. Shown in the *upper panel* are histograms of cell numbers (*y* axis) against DNA content (*x* axis) determined by measuring fluorescence intensity. Numbers denote the percentages of cells in the G0/G1, S, and G2/M phases. The experiment was repeated three times, and a statistical analysis is present in the *lower panel* (mean ± S.D.; *, $p < 0.05$; **, $p < 0.01$; ***, $p < 0.001$).

the expression of ARL2 at both the transcript and protein levels. The results demonstrate that our approach is a powerful tool for miRNA target identification.

A number of genetic studies suggest that ARL2 is involved in tubulin folding and plays a role in microtubule dynamics (24–30). In the present study, we showed that ARL2 had the potential to influence proliferation and cell cycle distribution in A549 cells. Moreover, we investigated whether the cellular phenotypes including migration, proliferation, and cell cycle arrest were regulated by miR-16 targeting ARL2. We showed that miR-16 could modulate cell migration by down-regulating genes other than ARL2, but that it negatively regulated proliferation and cell cycle progression from the G0/G1 phase to the S phase by silencing ARL2. However, siRNA against ARL2 only partially phenocopied the cellular phenotype of miR-16 on controlling cell cycle progression. One explanation for the more profound cell cycle arrest at the G0/G1 phase elicited by miR-16 rather than siRNA against ARL2 is that multiple cell cycle genes coordinately modulating cell cycle progression are targeted by miR-16. Indeed, several other cell cycle genes are regulated by miR-16, including CCND1, CCND3, CCNE1, CDK6, CARD10, and CDC27 (5–7). An emerging common theme is that multiple targets regulated by a single miRNA can act in concert, rather than individually, to regulate the same biological process. Coordinated regulation of many targets by a single miRNA may allow for a prompt cellular response to progress the cell cycle and also for rapid reversal of the miRNA-induced cell cycle regulation upon changes in miRNA synthesis, stability or localization. Taken together, our results combined with others demonstrate that the miR-16 family induces cell cycle arrest by silencing multiple downstream effectors simultaneously rather than an individual target.

In this study, we uncovered multiple targets of miR-16, including ARL2, by combining mRNA microarray profiles with bioinformatics analysis. We further experimentally validated ARL2 as a direct target of miR-16 and demonstrated that this targeting plays a critical role in regulating proliferation and cell cycle phenotypes.

REFERENCES

1. Ambros, V. (2004) *Nature* **431,** 350–355
2. Bartel, D. P. (2004) *Cell* **116,** 281–297
3. Calin, G. A., Dumitru, C. D., Shimizu, M., Bichi, R., Zupo, S., Noch, E., Aldler, H., Rattan, S., Keating, M., Rai, K., Rassenti, L., Kipps, T., Negrini, M., Bullrich, F., and Croce, C. M. (2002) *Proc. Natl. Acad. Sci. U. S. A.* **99,** 15524–15529
4. Cimmino, A., Calin, G. A., Fabbri, M., Iorio, M. V., Ferracin, M., Shimizu, M., Wojcik, S. E., Aqeilan, R. I., Zupo, S., Dono, M., Rassenti, L., Alder, H., Volinia, S., Liu, C. G., Kipps, T. J., Negrini, M., and Croce, C. M. (2005) *Proc. Natl. Acad. Sci. U. S. A.* **102,** 13944–13949
5. Linsley, P. S., Schelter, J., Burchard, J., Kibukawa, M., Martin, M. M., Bartz, S. R., Johnson, J. M., Cummins, J. M., Raymond, C. K., Dai, H., Chau, N., Cleary, M., Jackson, A. L., Carleton, M., and Lim, L. (2007) *Mol. Cell. Biol.* **27,** 2240–2252
6. Chen, R. W., Bemis, L. T., Amato, C. M., Myint, H., Tran, H., Birks, D. K., Eckhardt, S. G., and Robinson, W. A. (2008) *Blood* **112,** 822–829
7. Liu, Q., Fu, H., Sun, F., Zhang, H., Tie, Y., Zhu, J., Xing, R., Sun, Z., and Zheng, X. (2008) *Nucleic Acids Res.* **36,** 5391–5404
8. Jing, Q., Huang, S., Guth, S., Zarubin, T., Motoyama, A., Chen, J., Di Padova, F., Lin, S. C., Gram, H., and Han, J. (2005) *Cell* **120,** 623–634
9. Chen, C., Ridzon, D. A., Broomer, A. J., Zhou, Z., Lee, D. H., Nguyen, J. T., Barbisin, M., Xu, N. L., Mahuvakar, V. R., Andersen, M. R., Lao, K. Q., Livak, K. J., and Guegler, K. J. (2005) *Nucleic Acids Res.* **33,** e179
10. Tang, F., Hajkova, P., Barton, S. C., Lao, K., and Surani, M. A. (2006) *Nucleic Acids Res.* **34,** e9
11. Schmittgen, T. D., Jiang, J., Liu, Q., and Yang, L. (2004) *Nucleic Acids Res.* **32,** e43
12. Lewis, B. P., Shih, I. H., Jones-Rhoades, M. W., Bartel, D. P., and Burge, C. B. (2003) *Cell* **115,** 787–798
13. Krek, A., Grün, D., Poy, M. N., Wolf, R., Rosenberg, L., Epstein, E. J., MacMenamin, P., da Piedade, I., Gunsalus, K. C., Stoffel, M., and Rajewsky, N. (2005) *Nat. Genet.* **37,** 495–500
14. John, B., Enright, A. J., Aravin, A., Tuschl, T., Sander, C., and Marks, D. S. (2004) *PLoS Biol.* **2,** e363
15. Zhou, C., Cunningham, L., Marcus, A. I., Li, Y., and Kahn, R. A. (2006) *Mol. Biol. Cell* **17,** 2476–2487
16. Lim, L. P., Lau, N. C., Garrett-Engele, P., Grimson, A., Schelter, J. M., Castle, J., Bartel, D. P., Linsley, P. S., and Johnson, J. M. (2005) *Nature* **433,** 769–773
17. Yekta, S., Shih, I. H., and Bartel, D. P. (2004) *Science* **304,** 594–596
18. Sood, P., Krek, A., Zavolan, M., Macino, G., and Rajewsky, N. (2006) *Proc. Natl. Acad. Sci. U.S.A.* **103,** 2746–2751
19. Yu, Z., Raabe, T., and Hecht, N. B. (2005) *Biol. Reprod.* **73,** 427–433
20. Wu, L., Fan, J., and Belasco, J. G. (2006) *Proc. Natl. Acad. Sci. U.S.A.* **103,** 4034–4039
21. Selbach, M., Schwanhäusser, B., Thierfelder, N., Fang, Z., Khanin, R., and Rajewsky, N. (2008) *Nature* **455,** 58–63
22. Kahn, R. A., Kern, F. G., Clark, J., Gelmann, E. P., and Rulka, C. (1991) *J. Biol. Chem.* **266,** 2606–2614
23. Kahn, R. A., Volpicelli-Daley, L., Bowzard, B., Shrivastava-Ranjan, P., Li, Y., Zhou, C., and Cunningham, L. (2005) *Biochem. Soc. Trans.* **33,** 1269–1272
24. Antoshechkin, I., and Han, M. (2002) *Dev. Cell* **2,** 579–591
25. Hoyt, M. A., Macke, J. P., Roberts, B. T., and Geiser, J. R. (1997) *Genetics* **146,** 849–857
26. Radcliffe, P. A., Vardy, L., and Toda, T. (2000) *FEBS Lett.* **468,** 84–88
27. Bhamidipati, A., Lewis, S. A., and Cowan, N. J. (2000) *J. Cell Biol.* **149,** 1087–1096
28. McElver, J., Patton, D., Rumbaugh, M., Liu, C., Yang, L. J., and Meinke, D. (2000) *Plant Cell* **12,** 1379–1392
29. Sharer, J. D., Shern, J. F., Van Valkenburgh, H., Wallace, D. C., and Kahn, R. A. (2002) *Mol. Biol. Cell* **13,** 71–83
30. Shern, J. F., Sharer, J. D., Pallas, D. C., Bartolini, F., Cowan, N. J., Reed, M. S., Pohl, J., and Kahn, R. A. (2003) *J. Biol. Chem.* **278,** 40829–40836